Journal of Engineering Mathematics **30:** 119–130, 1996.

Image of a point force in a spherical container and its connection to the Lorentz reflection formula

CHRISTINE MAUL and SANGTAE KIM*
Bayer AG, ZF-TPT 3, Geb. E41, D-51368 Leverkusen, Germany; †*Dept. of Chemical Engineering, University of Wisconsin, Madison, WI 53706, USA*

Received 20 April 1995

Abstract. The image system for a velocity field of the Oseen tensor in a fluid region bounded by a rigid spherical container is derived. The Green's function and image system due to a nearby boundary constitute two themes explored in the pioneering (1896) paper by Lorentz. The special structure of our image system facilitates its incorporation as kernels for integral representations of velocity fields (another theme in the Lorentz paper) for a domain bounded by a spherical wall. The reflection formula for a plane wall is derived as a limiting case of the new solution.

1. Introduction

The 1896 paper by Lorentz [1] introduced the use of the Green's function (also known as the stokeslet, point force solution, or Oseen tensor) and integral representation for Stokes flow. In addition, Lorentz derived a reflection formula for handling the presence of a rigid planar wall; the formula converts an ambient Stokes velocity field in unbounded space, into one that satisfies the no-slip condition at the plane boundary. These themes can be combined, for example, to create the image system for the flow field of a point force next to a rigid planar wall, and to create an integral representation with a special kernel that automatically satisfies the boundary condition at a rigid planar wall, e.g. [2].

The one–hundred–year gap between Lorentz's classical paper and papers on low Reynolds number hydrodynamics of the modern era manifests itself in a number of ways, including, of course, the ubiquitous computer, and large-scale computations and simulations. The present authors certainly fit this mold; and yet, for this special occasion, it is perhaps more fitting to don the style of Lorentz, Oseen and others of a bygone era and consider the analyses of harmonic and biharmonic functions (especially if such analyses show some promise of leading to new computations that make more efficient use of high performance parallel supercomputers).

So in this paper we follow the themes pioneered by Lorentz, and consider special velocity representations generated by small particles in a fluid domain bounded by a rigid, spherical wall. Such geometries are of current interest in suspension rheology, including some recent work on spinning ball rheometry [3], and in biophysics as the basis for Brownian dynamics simulations in confined geometries.

For particles of dimension much smaller than the dimensions of the container, the first and natural approximation is to consider the particles as point forces and dipoles in the viscous fluid. For a more accurate description, we would then consider a distribution of such Stokes

* Correspondence concerning this article should be sent to Sangtae Kim.

singularities over the surface of the particles, i.e., an integral representation. Both approaches require the availability of a simple expression of the Green's function for this geometry.

The organization of this paper is as follows. As a prelude to the image system for a spherical container, we first revisit the image systems for a point force outside a rigid spherical particle (the exterior problem). The form of the solution provides a guide to our search of the solution for a point force inside a spherical container (the interior problem). Actually, both problems were solved by Oseen [4] but we shall see that for future applications, it is advantageous to recast his solutions as images of Stokes singularities. Such simplifications for the exterior problem were accomplished by Fuentes et al. [5,6]. More recently, Maul and Kim [7] have reported some progress on the interior problem, but were unable to find the line distributions or eliminate completely the so called Oseen vector harmonics. In the present work, these are accomplished.

Our singularity solution reveals an image system consisting of point forces, dipoles and quadrupoles, in contrast to the electrostatics analog for which a point charge inside a spherical cavity requires only an image charge outside the cavity. Furthermore, the presence of higher-order multipoles leads to a *reversal* in the orientation of the image stokeslet, as the placement of the original stokeslet is shifted from a point near the container wall to points closer to the center of the container.

For a stokeslet placed very close to the container wall, an asymptotic expansion of the present solution yields the solution for a point force near a plane wall. The form of that image immediately leads to a derivation of the Lorentz reflection formula for an incident Stokes flow field reflecting from a plane wall.

2. The exterior problem

Consider the Stokes flow field produced by a point force (or stokeslet) placed at an arbitrary but fixed point y outside a rigid spherical particle. The mathematical statement of this problem is:

$$-\nabla p + \mu \nabla^2 \boldsymbol{v} = -\boldsymbol{F}\delta(\boldsymbol{x}-\boldsymbol{y}), \tag{1}$$

$$\nabla \cdot \boldsymbol{v} = 0, \tag{2}$$

with the boundary condition, $\boldsymbol{v} = \boldsymbol{0}$ on the surface of the sphere. It is natural to proceed with a solution form that decomposes into a singular term and a regular term, i.e.,

$$\boldsymbol{v} = \frac{\boldsymbol{F}}{8\pi\mu} \cdot \mathcal{G}(\boldsymbol{x}-\boldsymbol{y}) + \boldsymbol{u} = \frac{\boldsymbol{F}}{8\pi\mu} \cdot \left[\frac{\delta}{r_{xy}} + \frac{(\boldsymbol{x}-\boldsymbol{y})(\boldsymbol{x}-\boldsymbol{y})}{r_{xy}^3} \right] + \boldsymbol{u}\,.$$

Here the first term (containing $\mathcal{G}$, the Oseen tensor) is the Green's function for the unbounded domain and is thus singular at $\boldsymbol{x} = \boldsymbol{y}$. We shall use $r_{xy} = |\boldsymbol{x}-\boldsymbol{y}|$ to denote the distance from any point $\boldsymbol{x}$ in the fluid domain to the location of the singularity, as shown in Fig. 1. Note that lengths have been scaled by the sphere radius, so that the sphere has a unit radius.

As mentioned before, this problem, and the closely related one of a stokeslet inside a rigid spherical container, were first solved by Oseen and presented in his 1927 book, *Hydrodynamik*. In the interest of brevity, his somewhat lengthy solution is not reproduced here. We should also note that notable extensions to Oseen's work, generally known as sphere theorems, have been developed [8,9,10,11], but these do not lend themselves in a straightforward fashion to our computational project on Stokes flows that are generated by the motion of multiple particles

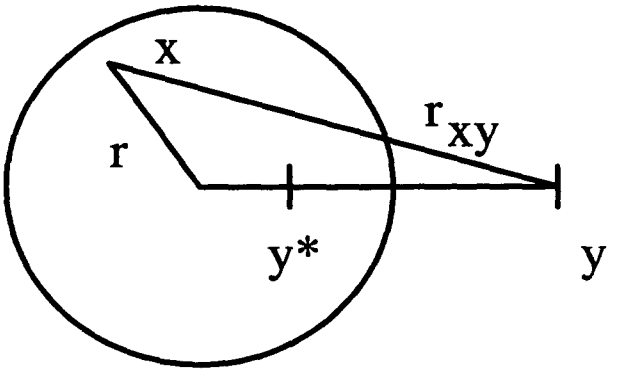

Fig. 1. The stokeslet and sphere geometry.

in a spherical domain. Instead, for our purposes, it is advantageous to write the solution as an image system of Stokes singularities as in Fuentes et al. [5,6]. We first decompose the external force $\boldsymbol{F}$ acting at the stokeslet location y into axisymmetric and asymmetric (transverse) components,

$$\boldsymbol{F} = \boldsymbol{F}^{\parallel} + \boldsymbol{F}^{\perp} = \boldsymbol{F} \cdot ee + \boldsymbol{F} \cdot (\delta - ee) ,$$

where the unit vector $e = \boldsymbol{y}/|\boldsymbol{y}| = \boldsymbol{y}/y$ is directed along the axis from the sphere center (taken to be the origin) to the location of the stokeslet. The character of the solution is quite distinct for the two cases which are as follows:

$$\begin{aligned} \boldsymbol{u}^{\parallel} = & -(\frac{3}{2}y^{-1} - \frac{1}{2}y^{-3})\boldsymbol{F}^{\parallel} \cdot \frac{\mathcal{G}(\boldsymbol{x} - \boldsymbol{y}^*)}{8\pi\mu} + (y^{-2} - y^{-4})(\boldsymbol{F}^{\parallel} e \cdot \nabla) \cdot \frac{\mathcal{G}(\boldsymbol{x} - \boldsymbol{y}^*)}{8\pi\mu} \\ & - \frac{1}{4}y^{-1}(1 - y^{-2})^2 \boldsymbol{F}^{\parallel} \cdot \nabla^2 \frac{\mathcal{G}(\boldsymbol{x} - \boldsymbol{y}^*)}{8\pi\mu} , \end{aligned} \tag{3}$$

$$\begin{aligned} \boldsymbol{u}^{\perp} = & -(\frac{3}{2}y^{-1} - \frac{1}{2}y^{-3})\boldsymbol{F}^{\perp} \cdot \frac{\mathcal{G}(\boldsymbol{x} - \boldsymbol{y}^*)}{8\pi\mu} - [(y^{-2} - y^{-4})\boldsymbol{F}^{\perp}(e \cdot \nabla)] \cdot \frac{\mathcal{G}(\boldsymbol{x} - \boldsymbol{y}^*)}{8\pi\mu} \\ & + \frac{1}{4}y^{-1}(1 - y^{-2})^2 \boldsymbol{F}^{\perp} \cdot \frac{\nabla^2 \mathcal{G}(\boldsymbol{x} - \boldsymbol{y}^*)}{8\pi\mu} - 2y^{-2}(1 - y^{-2}) \frac{\boldsymbol{F}^{\perp} \times e}{8\pi\mu} \times \nabla \frac{1}{|\boldsymbol{x} - \boldsymbol{y}^*|} \\ & + \frac{3}{2}(y - y^{-1}) \int_0^{1/y} \xi \boldsymbol{F}^{\perp} \cdot \left[1 - \frac{1}{2}(1 - \xi^2)\nabla^2\right] \frac{\mathcal{G}(\boldsymbol{x} - \boldsymbol{\xi})}{8\pi\mu} \, \mathrm{d}\xi \\ & + 3(y - y^{-1}) \int_0^{1/y} \xi^2 \frac{\boldsymbol{F}^{\perp} \times e}{8\pi\mu} \times \nabla \frac{\mathrm{d}\xi}{|\boldsymbol{x} - \boldsymbol{\xi}|} . \end{aligned} \tag{4}$$

Thus for a stokeslet outside a rigid sphere, Oseen's solution can be rewritten as a collection of stokeslets, stresslets, rotlets and degenerate Stokes quadrupoles located inside the spherical particle. It is interesting to compare this with the simpler situation in potential theory (electrostatics); a point charge at y next to a spherical conductor has an image consisting of just an image charge at y^*. This in turn implies that, for electrostatics,the image approach solves simultaneously the interior as well as the exterior problem. The above solution shows that this nice situation does not extend to the biharmonic equation for Stokes flow.

3. The Interior Problem

3.1. Oseen's solution Written with Stokes singularities

As mentioned before, Oseen [4] has already solved the interior problem,

$$-\nabla p + \mu\nabla^2 \boldsymbol{v} \;=\; -\boldsymbol{F}\delta(\boldsymbol{x}-\boldsymbol{y}^*)\,, \qquad \nabla\cdot\boldsymbol{v}=0\,,$$

with the boundary condition, $\boldsymbol{v}=\boldsymbol{0}$ on the surface of the spherical container. Oseen's solution is a lengthy expression that is written in terms of vector harmonics. Recently, Maul and Kim [7] showed that the interior problem has a simpler singularity form. They use exactly the same geometry as in Fig. 1, but now interpret $\boldsymbol{y}^*$ as the location of a stokeslet in the fluid region bounded by a spherical container, and $\boldsymbol{y}$ as the location of the image singularities. For the axisymmetric case, they discovered a simple "short cut", namely the superposition of the image systems for three exterior problems leads to an image that is just a stokeslet at $\boldsymbol{y}^*$! They thus arrived at the solution to the interior problem,

$$\boldsymbol{v} = \boldsymbol{F}^{\parallel}\cdot\frac{\mathcal{G}(\boldsymbol{x}-\boldsymbol{y}^*)}{8\pi\mu} + \boldsymbol{u}^{\parallel,\mathrm{int}}\,,$$

with

$$\begin{aligned}\boldsymbol{u}^{\parallel,\mathrm{int}} \;=\; & \frac{y^3-3y}{2}\boldsymbol{F}^{\parallel}\cdot\frac{\mathcal{G}(\boldsymbol{x}-\boldsymbol{y})}{8\pi\mu} - y^2(y^2-1)(\boldsymbol{F}^{\parallel}\boldsymbol{e}\cdot\nabla)\cdot\frac{\mathcal{G}(\boldsymbol{x}-\boldsymbol{y})}{8\pi\mu} \\ & - \frac{1}{4}y(y^2-1)^2\boldsymbol{F}^{\parallel}\cdot\frac{\nabla^2\mathcal{G}(\boldsymbol{x}-\boldsymbol{y})}{8\pi\mu}\,. \end{aligned} \tag{5}$$

The situation for the asymmetric (transverse) stokeslet (with $\boldsymbol{F}^{\perp}\cdot\boldsymbol{e}=0$) is not as simple. In addition to the interior singularities that were employed in the axisymmetric problem, the asymmetric stokeslet requires a distribution of rotlets and skewed quadrupoles (i.e., $(\boldsymbol{e}\cdot\nabla)$ acting on a rotlet). Furthermore, we anticipate line distributions of singularities from $\boldsymbol{y}$ to ∞.

Maul and Kim [7] have shown that Oseen's solution can be written as

$$\begin{aligned}\boldsymbol{u}^{\perp,\mathrm{int}} \;=\; & \frac{3y-5y^3}{2}\boldsymbol{F}^{\perp}\cdot\frac{\mathcal{G}(\boldsymbol{x}-\boldsymbol{y})}{8\pi\mu} + \frac{y(y^2-1)^2}{4}\boldsymbol{F}^{\perp}\cdot\frac{\nabla^2\mathcal{G}(\boldsymbol{x}-\boldsymbol{y})}{8\pi\mu} \\ & + y^2(y^2-1)\,(\boldsymbol{e}\boldsymbol{F}^{\perp}\cdot\nabla)\cdot\frac{\mathcal{G}(\boldsymbol{x}-\boldsymbol{y})}{8\pi\mu} \\ & + 3y(y^2-1)\,\frac{1}{8\pi\mu}\,\frac{\boldsymbol{F}^{\perp}}{r_{xy}} + (r^2-1)\,\frac{1}{8\pi\mu}\,\nabla(\boldsymbol{F}^{\perp}\cdot\boldsymbol{\varphi})\,, \end{aligned} \tag{6}$$

with $r=|\boldsymbol{x}|$ and the vector harmonic $\boldsymbol{\varphi}$ given by

$$\boldsymbol{\varphi} = \frac{3y(y^2-1)}{2}\,\frac{\boldsymbol{x}}{r_{xy}}\,\frac{r-y\cos\vartheta+r_{xy}\cos\vartheta}{r\,y^2\sin^2\vartheta}\,. \tag{7}$$

Here ϑ is the angle between $\boldsymbol{e}$ and $\boldsymbol{x}$. So their first attempt at a singularity solution was not completely successful. The first term on the last line of Eq. (6) is not a solenoidal field, hence the appearance of the Oseen–type vector harmonic $\boldsymbol{\varphi}$. Taken together, the two terms on the last line do satisfy the Stokes equations as explained in [7]. Their solution represents an advance

in the sense that the expression for φ is far simpler than the one proposed in Oseen [4], thanks to the use of Stokes singularities at y. We now complete the story by showing that the φ can be represented as a line distribution of singularities from the image point y to ∞.

3.2. VECTOR HARMONIC AS A LINE DISTRIBUTION OF SINGULARITIES

We start with the last line of Eq. (6) and define a vector field

$$U_j = \frac{F_j^\perp}{r_{xy}} + (r^2 - 1)F_k^\perp \frac{\partial \psi_k}{\partial x_j} .$$

By applying $\partial/\partial x_\ell$ twice to this expression, we conclude that its pressure field is

$$p = 2\mu F_k^\perp (\psi_k + 2x_\ell \frac{\partial \psi_k}{\partial x_\ell}) ,$$

while the continuity condition $U_{j,j} = 0$ requires

$$\frac{\partial}{\partial x_j}\left(\frac{F_j^\perp}{r_{xy}}\right) + 2x_j F_k^\perp \frac{\partial \psi_k}{\partial x_j} = 0 . \tag{8}$$

Note that this implies that the expression for the pressure simplifies to: $p = 2\mu \boldsymbol{F}^\perp \cdot (\psi - \nabla r_{xy}^{-1})$. Following Oseen, we express the continuity condition, Eq. (8), in spherical polar coordinates:

$$F_k^\perp r \frac{\partial \psi_k}{\partial r} = -\frac{1}{2}\frac{\partial}{\partial x_k}\left(\frac{F_k^\perp}{r_{xy}}\right) .$$

At this point, we employ the Legendre expansion to express $1/r_{xy}$ in terms of interior harmonics about the sphere center:

$$\frac{1}{r_{xy}} = \sum_{n=0}^{\infty} \frac{r^{2n+1}}{y^{n+1}} \frac{(-e\cdot\nabla)^n}{n!}\frac{1}{r} = \frac{1}{y} + \frac{e\cdot x}{y^2} + \sum_{n=2}^{\infty} \frac{r^{2n+1}}{y^{n+1}} \frac{(-e\cdot\nabla)^n}{n!}\frac{1}{r} .$$

The first term ($n = 0$) is annihilated upon operation by $F_k^\perp(\partial/\partial x_k)$ because it is a constant, while the second term ($n = 1$) is annihilated by the same operator because $F_k^\perp e_k = 0$; thus we arrive at the relation,

$$F_k^\perp r \frac{\partial \psi_k}{\partial r} = -\frac{F_k^\perp}{2}\frac{\partial}{\partial x_k} \sum_{n=2}^{\infty} \frac{r^{2n+1}}{y^{n+1}} \frac{(-e\cdot\nabla)^n}{n!}\frac{1}{r} .$$

Now each term in the RHS is a harmonic of degree $n - 1$ (keep in mind that the nabla operator outside the summation reduces the degree from n to $n-1$). Since for h_{n-1} a harmonic of degree $n - 1$ we have $r(\partial/\partial r)h_{n-1} = (n-1)h_{n-1}$ we arrive at the following expression for ψ_k:

$$F_k^\perp \psi_k = -\frac{F_k^\perp}{2}\frac{\partial}{\partial x_k} \sum_{n=2}^{\infty} \frac{1}{(n-1)} \frac{r^{2n+1}}{y^{n+1}} \frac{(-e\cdot\nabla)^n}{n!}\frac{1}{r} .$$

This is a perfectly valid expression for Oseen's vector harmonic, but we shall proceed to a formulation in terms of a line integral.

Let ξ be a point on the axis, with $\xi = |\xi| \geqslant y$ as shown in Fig. 1, and construct the Legendre expansion for the harmonic $|x - \xi|^{-1}$. Multiply both sides by ξ, and apply the operator $F_k^{\perp}(\partial/\partial x_k)$ to both sides. This leads to the relation:

$$F_k^{\perp} \frac{\partial}{\partial x_k} \frac{\xi}{|x-\xi|} = F_k^{\perp} \frac{\partial}{\partial x_k} \sum_{n=2}^{\infty} \frac{r^{2n+1}}{\xi^n} \frac{(-e \cdot \nabla)^n}{n!} \frac{1}{r} .$$

Integrate this relation with respect to ξ from y to ∞:

$$\begin{aligned} \int_y^{\infty} F_k^{\perp} \frac{\partial}{\partial x_k} \frac{\xi}{|x-\xi|} \, d\xi &= \int_y^{\infty} F_k^{\perp} \frac{\partial}{\partial x_k} \sum_{n=2}^{\infty} \frac{r^{2n+1}}{\xi^n} \frac{(-e \cdot \nabla)^n}{n!} \frac{1}{r} \, d\xi \\ &= F_k^{\perp} \frac{\partial}{\partial x_k} \sum_{n=2}^{\infty} \frac{1}{(n-1)} \frac{r^{2n+1}}{y^{n-1}} \frac{(-e \cdot \nabla)^n}{n!} \frac{1}{r} \\ &= -2y^2 F_k^{\perp} \psi_k . \end{aligned}$$

In this manner, we arrive at the desired result,

$$F_k^{\perp} \psi_k = \frac{-1}{2y^2} \int_y^{\infty} F_k^{\perp} \frac{\partial}{\partial x_k} \frac{\xi}{|x-\xi|} \, \mathrm{d}\xi = \frac{F_k^{\perp} x_k}{2y^2} \int_y^{\infty} \frac{\xi}{|x-\xi|^3} \, \mathrm{d}\xi . \tag{9}$$

In the Appendix, we work out expressions for integrals of the form

$$L_{mn} = \int_y^{\infty} \frac{\xi^m \, \mathrm{d}\xi}{|x-\xi|^n} .$$

Upon substitution of the expression for L_{13} in ψ_k we obtain

$$F_k^{\perp} \psi_k = \frac{F_k^{\perp} x_k}{2y^2} \times \begin{cases} \frac{1}{r_{xy}} + \frac{r}{2r_{xy}^2} & \text{if } \vartheta = 0, \\ \frac{1}{r_{xy}} + \frac{\cos\vartheta}{r\sin^2\vartheta} \left(1 - \frac{y - r\cos\vartheta}{r_{xy}}\right) & \text{if } 0 < \vartheta < \pi, \\ \frac{1}{r_{xy}} - \frac{r}{2r_{xy}^2} & \text{if } \vartheta = \pi . \end{cases}$$

The degenerate cases $\vartheta = 0$ and $\vartheta = \pi$ can be obtained by taking limits in the general expression, or more easily by putting x on the axis and evaluating the line integral. We also work out the derivative that appears in the velocity expression,

$$F_k^{\perp} \frac{\partial \psi_k}{\partial x_j} = \frac{F_j^{\perp}}{2y^2} \int_y^{\infty} \frac{\xi}{|x-\xi|^3} \, \mathrm{d}\xi - \frac{3F_k^{\perp} x_k}{2y^2} \int_y^{\infty} \frac{\xi(x_j - \xi e_j)}{|x-\xi|^5} \, \mathrm{d}\xi . \tag{10}$$

This expression requires L_{15} and L_{25} as provided in the Appendix.

We now check our result by reattaching the extra constant factor onto ψ_k:

$$\begin{aligned} F_k^{\perp} \varphi_k &= 3y(y^2-1) F_k^{\perp} \psi_k \\ &= 3y(y^2-1) \frac{F_k^{\perp} x_k}{2y^2} \left[\frac{1}{r_{xy}} + \frac{\cos\vartheta}{r\sin^2\vartheta} \left(1 - \frac{y - r\cos\vartheta}{r_{xy}}\right) \right] \\ &= 3y(y^2-1) \frac{F_k^{\perp} x_k}{2y^2 r_{xy}} \frac{r + r_{xy}\cos\vartheta - y\cos\vartheta}{r\sin^2\vartheta} , \end{aligned}$$

and this is indeed the same as Eq. (7).

In summary, the image solution for the asymmetric stokeslet is:

$$\begin{aligned}\boldsymbol{u}^{\perp,\mathrm{int}} &= \frac{3y-5y^3}{2}\boldsymbol{F}^{\perp}\cdot\frac{\mathcal{G}(x-y)}{8\pi\mu} + \frac{y(y^2-1)^2}{4}\boldsymbol{F}^{\perp}\cdot\frac{\nabla^2\mathcal{G}(x-y)}{8\pi\mu}\\ &+ y^2(y^2-1)\,(e\boldsymbol{F}^{\perp}\cdot\nabla)\cdot\frac{\mathcal{G}(x-y)}{8\pi\mu}\\ &+ 3y(y^2-1)\,\frac{1}{8\pi\mu}\,\frac{\boldsymbol{F}^{\perp}}{r_{xy}}\\ &+ (r^2-1)\,\frac{3y(y^2-1)}{8\pi\mu}\left[\frac{\boldsymbol{F}^{\perp}}{2y^2}\int_y^{\infty}\frac{\xi\,\mathrm{d}\xi}{|x-\xi|^3} - \frac{3\boldsymbol{F}^{\perp}\cdot x}{2y^2}\int_y^{\infty}\frac{\xi(x-\xi e)}{|x-\xi|^5}\,\mathrm{d}\xi\right],\end{aligned} \tag{11}$$

and we have achieved our goal of a simple singularity solution form. The integrals can be evaluated analytically and expressed in terms of the L_{mn} functions of the appendix or, in the case of kernels for boundary integral computations of large simulations on massively parallel computer architectures, by dataparallel implementations of Gaussian quadrature rules.

The general solution to the interior problem is obtained by a linear combination of Eqs. (5) and (12) and is presented in the Appendix.

It should be noted that in Eq. (12) the terms from the vector harmonic (terms on the last two lines) are not in the form of Stokes singularities. It is possible to manipulate these two terms into Stokesian images of the form:

$$\frac{3(y^2-1)}{2y}\left[\int_y^{\infty}\xi\boldsymbol{F}^{\perp}\cdot\frac{\mathcal{G}(x-\xi)}{8\pi\mu}\,\mathrm{d}\xi + \boldsymbol{F}^{\perp}\cdot\frac{\mathcal{G}(x-y)}{8\pi\mu}\right],$$

plus additional line distributions of degenerate quadrupoles and rotlets in analogy with the exterior solution. One possible pathway for the derivation of such expressions consists of addition theorems for Stokes singularities at a point ξ on the line distribution as given in Chapter 10 of [12], integration of the resulting identities with respect to ξ from y to ∞, and matching of the coefficients of the basis set for the vector harmonics. However, these alternate forms are of limited utility in future work because the (floating point) operation counts would increase.

3.3. Further comments on the analogy with electrostatics

As is now evident, the image system for the viscous hydrodynamic problem shares some similarities with, but possesses key differences from that of the electrostatics problem. The differences are further highlighted by a phenomenon that we could call "stokeslet reversal." Consider Eq. (5) for the image of an interior stokeslet located at y^*. When the stokeslet is very close to the wall, we may write $y = 1+\epsilon$ and $y^* = 1/y \sim 1-\epsilon$, with $\epsilon \ll 1$, and we obtain the expected result that the image stokeslet is equal in magnitude but pointed in the opposite direction from the original stokeslet. However, for $y > \sqrt{3}$, i.e. $y^* < \sqrt{3}/3$, the sign of the image stokeslet is opposite to that obtained from physical intuition and at the critical value of $y = \sqrt{3}$, $y^* = \sqrt{3}/3$, the image stokeslet vanishes! Of course, in all cases, the net flow produced by the total image system must cancel the flow of the original stokeslet. Stokeslet reversal is mathematically feasible only because of the presence of the other singularities. This point is brought out quite clearly in the expression for v on the container wall at the point

that intersects the line segment between y^* and y (i.e. where $\vartheta = 0$):

$$\text{Image stokeslet velocity} = \frac{y^3 - 3y}{y-1}\frac{F^{\|}}{8\pi\mu},$$

$$\text{Image dipole velocity} = -\frac{2y^3 + 2y^2}{y-1}\frac{F^{\|}}{8\pi\mu},$$

$$\text{Image quadrupole velocity} = \frac{y^3 + 2y^2 + y}{y-1}\frac{F^{\|}}{8\pi\mu}.$$

For all y, the total flow from all images will cancel the field of the stokeslet at y^*,

$$\text{Original stokeslet velocity} = \frac{2y}{y-1}\frac{F^{\|}}{8\pi\mu},$$

but the flow from just the image stokeslet exhibits a reversal at $y = \sqrt{3}$.

The above reversal effect can be eliminated if we use simple integration to obtain the identity,

$$\int_y^\infty -(e\cdot\nabla)\frac{\mathcal{G}(x-\xi)}{8\pi\mu}\,\mathrm{d}\xi = \int_y^\infty \frac{\partial}{\partial\xi_3}\frac{\mathcal{G}(x-\xi)}{8\pi\mu}\,\mathrm{d}\xi = -\frac{\mathcal{G}(x-y)}{8\pi\mu}.$$

The singularity solution, Eq. (5), may then be rearranged as

$$\begin{aligned} u^{\|,\mathrm{int}} &= -yF^{\|}\cdot\frac{\mathcal{G}(x-y)}{8\pi\mu} - y^2(y^2-1)(F^{\|}e\cdot\nabla)\cdot\frac{\mathcal{G}(x-y)}{8\pi\mu} \\ &\quad - \frac{1}{4}y(y^2-1)^2F^{\|}\cdot\frac{\nabla^2\mathcal{G}(x-y)}{8\pi\mu} + \frac{1}{2}y(y^2-1)\int_y^\infty (F^{\|}e\cdot\nabla)\cdot\frac{\mathcal{G}(x-\xi)}{8\pi\mu}\,\mathrm{d}\xi. \end{aligned}$$

The coefficient of the image stokeslet now preserves its sign for all y with $y > 0$, but the price is an image system with a line distribution.

3.4. The Lorentz wall reflection formula

We now go back to the problem of the stokeslet very close to the container wall, and set $y = 1 + \epsilon$, $\epsilon \ll 1$. As explained in Chapter 12 of [12, pp. 239–261] the image system should then approach that of the plane wall; the expressions simplify to leading order as:

$$\begin{aligned} u^{\mathrm{int}} &= -(F^{\perp} + F^{\|})\cdot\frac{\mathcal{G}(x-y)}{8\pi\mu} - 2\epsilon[(F^{\perp} - F^{\|})\cdot\nabla]n\cdot\frac{\mathcal{G}(x-y)}{8\pi\mu} \\ &\quad + \epsilon^2(F^{\perp} - F^{\|})\cdot\frac{\nabla^2\mathcal{G}(x-y)}{8\pi\mu}, \end{aligned} \tag{12}$$

where $n = -e$ (pointing into the fluid) is the normal for the plane wall. Note that ϵ is now the distance from the plane and y^* is now the mirror image of y.

Although Eq. 12 is a valid expression for the image system it is not difficult to convert it to the following alternate expression in which the geometric parameter ϵ does not appear explicitly:

$$u^{\mathrm{int}} = -(\delta - 2nn)\cdot u^{\mathrm{mir}} - 2n\cdot x\nabla(n\cdot u^{\mathrm{mir}}) + (n\cdot x)^2\nabla^2 u^{\mathrm{mir}}, \tag{13}$$

where

$$\boldsymbol{u}^{\mathrm{mir}} = (\boldsymbol{F}^{\perp} - \boldsymbol{F}^{\parallel}) \cdot \frac{\mathcal{G}(\boldsymbol{x} - \boldsymbol{y})}{8\pi\mu} \tag{14}$$

is the *mirror image* of the original stokeslet. Eq. (13) is the image solution of Lorentz [1].

We have thus arrived at the Lorentz reflection principle, as applied to the free space Green's function:

1. Create the mirror reflection of the original flow field,
   $\boldsymbol{u}^{\mathrm{mir}}(x, y, z) = \mathcal{M}(\boldsymbol{u}) = (\delta - ee) \cdot \boldsymbol{u}(x, y, -z)$,
   where $\mathcal{M}$ denotes the mirror operator with the mirror placed on the XY–plane.
2. Create the reflected field by applying a second operator, $\mathcal{L}$, with its definition motivated by Eq. (13),
   $\mathcal{L}(\boldsymbol{u}) = -(\delta - 2nn) \cdot \boldsymbol{u} - 2n \cdot \boldsymbol{x}\nabla(n \cdot \boldsymbol{u}) + (n \cdot \boldsymbol{x})^2\nabla^2\boldsymbol{u}$.

What applies to the free space Green's function should apply to all Stokes flows, so we arrive at Lorentz's conclusion: *given a Stokes velocity field $\boldsymbol{u}$ defined everywhere in R^3, the reflection from a plane wall is given by* $\mathcal{L}\mathcal{M}(\boldsymbol{u})$.

We conclude this section with a brief discussion of the theory for the reflection from the spherical container. We assume that the disturbance flow field in the container is created by some small particle, with the particle represented by a set of Stokes singularities. Examples of such representations are discussed in Chapter 3 of [12, pp. 47–72] for spheres, spheroids, ellipsoids and slender bodies. For each singularity, we compute the image field, $\boldsymbol{u}$, as discussed earlier. The dampening effect of the container boundary on the mobility of the particle may then be computed by the so called first reflection [12, pp. 311–319 and 13, pp 240–270] which consists of an application of the Faxén relation with $\boldsymbol{u}$ as the incident field.

For the completely general treatment of particle hydrodynamics within the spherical container (arbitrary particle shape, many–body effects, etc.), the Stokes singularities would be distributed over the particle surface, i.e., we would employ an integral representation. In contrast to Oseen's expression, it is relatively straightforward to compute the stress and traction fields of the image systems presented in Eqs. (5) and (6), and thus derive the kernels of the relevant boundary integral equations (the table of integrals in the appendix needs to be augmented with expressions for L_{m7}). This then leads us to the many–body simulations as in [14].

4. Conclusion

We have shown that the image of a point force inside a rigid spherical container consists of stokeslets, Stokes dipoles and degenerate Stokes quadrupoles located at the image point (for the axisymmetric and asymmetric problem) plus (for the asymmetric case only) a vector harmonic that can be represented as a simple line distribution of singularities from the image point to infinity. These new expressions are especially useful for boundary integral formulations that are based on special kernels that satisfy the no-slip condition at the container wall. In such computations, dataparallel implementations of Gaussian quadrature rules are more efficient than the analytic formulae for the line integrals. The recent work by Traenkle et al. [15] explores in greater detail the utility of boundary integral equations with special kernels as a function of different parallel computer architectures.

The presence of higher-order multipoles in the image system points out the subtle difference between the harmonic and biharmonic equations; some of the simplicity of the image system

from potential theory is lost. For example, because of the contributions from the higher order multipoles, there is a *reversal* in the orientation of the image stokeslet, as the parameter y^* for the location of the stokeslet goes through the critical radius $\sqrt{3}/3 = 0.577...$. The reversal effect may be eliminated, but only by admitting line distributions in the image system of the axisymmetric problem.

Our solution for the image goes smoothly to that for a point force near a plane wall, when the stokeslet is placed near the container boundary. The utility of the image approach is demonstrated by showing the pathway to Lorentz's reflection formula for an incident Stokes flow field reflecting from a plane wall, and by the streamlined process for the derivation of kernels for boundary integral representations.

Acknowledgments

This material is based on work supported by the National Science Foundation Grant CTS-9218668 and the Office of Naval Research Grant N00014–92–J–1564.

Appendix

This appendix contains the expression for the Green's dyadic for the general orientation of the point force $\boldsymbol{F}$ and expressions for the line integrals

$$L_{mn} = \int_y^\infty \frac{\xi^m \, \mathrm{d}\xi}{|x - \xi|^n}$$

that appear in the formulae for φ_k and its derivatives. We consider first the line integrals. We let

$$x = (r \sin\vartheta \cos\phi, r \sin\vartheta \sin\phi, r \cos\vartheta) \,, \quad \xi = (0, 0, \xi) \,,$$

$$|x - \xi| = \sqrt{r^2 \sin^2\vartheta + (\xi - r\cos\vartheta)^2} \,.$$

By setting

$$u = (\xi/r) - \cos\vartheta \,, \quad \mathrm{d}u = \mathrm{d}\xi/r \,, \quad Z = \frac{y}{r} - \cos\vartheta \,,$$

the integrals may be rendered to a more convenient form

$$r^{m+1-n} \int_Z^\infty \frac{(u + \cos\vartheta)^m \, \mathrm{d}u}{(\sin^2\vartheta + u^2)^{n/2}}$$

that is more easily evaluated. The final results are given in Table 1.

We now consider the Green's function with an arbitrary orientation of the point force. In index notation, the components of the force are written as

$$F_k = F_k^{\parallel} + F_k^{\perp} = e_k e_m F_m + (\delta_{km} - e_k e_m) F_m \,.$$

We insert these representations into the axisymmetric and asymmetric cases to obtain the desired result for the Green's dyadic:

$$\left\{ \mathcal{G}_{jm}(x - y^*) + \overline{\mathcal{G}}_{jm}(x) \right\} \frac{F_m}{8\pi\mu}$$

Table 1. Expressions for the integrals L_{mn}. Here $Z = (y/r) - \cos\vartheta$.

$$L_{mn} = \int_y^\infty \frac{\xi^m \,\mathrm{d}\xi}{|x-\xi|^n} = r^{m+1-n} \int_Z^\infty \frac{(u+\cos\vartheta)^m \,\mathrm{d}u}{(\sin^2\vartheta + u^2)^{n/2}}$$

$$rL_{13} = \begin{cases} = \frac{r}{r_{xy}} + \frac{r^2}{2r_{xy}^2} & \text{if } \vartheta = 0, \\ = \frac{r}{r_{xy}} + \frac{\cos\vartheta}{\sin^2\vartheta}\left(1 - Z\frac{r}{r_{xy}}\right) & \text{if } 0 < \vartheta < \pi, \\ = \frac{r}{r_{xy}} - \frac{r^2}{2r_{xy}^2} & \text{if } \vartheta = \pi\,. \end{cases}$$

$$r^3 L_{15} = \begin{cases} = \frac{r^3}{3r_{xy}^3} + \frac{r^4}{4r_{xy}^4} & \text{if } \vartheta = 0, \\ = \frac{r^3}{3r_{xy}^3} - \frac{\cos\vartheta}{3\sin^2\vartheta} Z \frac{r^3}{r_{xy}^3} + \frac{2\cos\vartheta}{3\sin^4\vartheta}\left(1 - Z\frac{r}{r_{xy}}\right) & \text{if } 0 < \vartheta < \pi, \\ = \frac{r^3}{3r_{xy}^3} - \frac{r^4}{4r_{xy}^4} & \text{if } \vartheta = \pi\,. \end{cases}$$

$$r^2 L_{25} = \begin{cases} = \frac{r^2}{2r_{xy}^2} + \frac{2}{3}\frac{r^3}{r_{xy}^3} + \frac{r^4}{4r_{xy}^4} & \text{if } \vartheta = 0, \\ = \frac{2}{3}\cos\vartheta \frac{r^3}{r_{xy}^3} + \frac{Z}{3}\frac{r^3}{r_{xy}^3} - \frac{1}{\sin^2\vartheta}\left(\frac{1}{3} + \frac{1}{3}Z\frac{r}{r_{xy}} + \frac{\cos^2\vartheta}{3} Z \frac{r^3}{r_{xy}^3}\right) & \\ \quad + \frac{2}{3\sin^4\vartheta}\left(1 - \cos^2\vartheta\, Z\frac{r}{r_{xy}}\right) & \text{if } 0 < \vartheta < \pi, \\ = \frac{r^2}{2r_{xy}^2} - \frac{2}{3}\frac{r^3}{r_{xy}^3} + \frac{r^4}{4r_{xy}^4} & \text{if } \vartheta = \pi\,. \end{cases}$$

with

$$\begin{aligned} \overline{\mathcal{G}}_{jm}(\boldsymbol{x}) \;=\; & e_m e_k \left\{ \frac{y^3 - 3y}{2} \mathcal{G}_{jk}(\boldsymbol{x}-\boldsymbol{y}) - y^2(y^2-1) e_\ell \mathcal{G}_{jk,\ell}(\boldsymbol{x}-\boldsymbol{y}) \right. \\ & \left. - \frac{1}{4} y (y^2-1)^2 \nabla^2 \mathcal{G}_{jk}(\boldsymbol{x}-\boldsymbol{y}) \right\} \\ & + (\delta_{km} - e_k e_m) \left\{ \frac{3y - 5y^3}{2} \mathcal{G}_{jk}(\boldsymbol{x}-\boldsymbol{y}) + \frac{y(y^2-1)^2}{4} \nabla^2 \mathcal{G}_{jk}(\boldsymbol{x}-\boldsymbol{y}) \right\} \\ & + y^2(y^2-1)\, e_k (\delta_{\ell m} - e_\ell e_m)\, \mathcal{G}_{jk,\ell}(\boldsymbol{x}-\boldsymbol{y}) \\ & + 3y(y^2-1) \frac{(\delta_{jm} - e_j e_m)}{r_{xy}} \\ & + (r^2-1)\, 3(y^2-1) \left[\frac{(\delta_{jm} - e_j e_m)}{2y} \int_y^\infty \frac{\xi \,\mathrm{d}\xi}{|\boldsymbol{x}-\boldsymbol{\xi}|^3} \right. \\ & \left. - \frac{3(\delta_{km} - e_k e_m) x_k}{2y} \int_y^\infty \frac{\xi (x_j - \xi e_j)}{|\boldsymbol{x}-\boldsymbol{\xi}|^5} \,\mathrm{d}\xi \right] . \end{aligned}$$

5. Notes

[1]the displayed terms produce the pressure field that was discussed just after Eq. (8).

[2]The $\parallel$ and $\perp$ designations are still relative to the symmetry axis, so that for example $\perp$ is *not* orientation normal to the plane.

References

1. H.A. Lorentz, A general theorem concerning the motion of a viscous fluid and a few consequences derived from it. *Versl. Konigl. Akad. Wetensch. Amst.* 5 (1896) 168–175.
2. C. Maul, S. Kim, V. Ilic, D. Tullock and N. Phan-Thien, Sedimentation of hexagonal flakes in a half-space: numerical predictions and experiments in Stokes flow. *J. Imaging Science and Technology* 38 (1994) 241–248.
3. L.A. Mondy et al. Spinning ball rheometry. *Soc. Rheology Annual Meeting* October (1994), Philadelphia.
4. C.W. Oseen, *Hydrodynamik* (see pp. 97–107) Leipzig: Akad. Verlagsgesellschaft, (1927) 337 pp.
5. Y.O. Fuentes, S. Kim and D.J. Jeffrey, Mobility functions for two unequal viscous drops in Stokes flow. I. Axisymmetric motions. *Phys. Fluids* 31 (1988) 2445–2455.
6. Y.O. Fuentes, S. Kim and D.J. Jeffrey, Mobility functions for two unequal viscous drops in Stokes flow. II. Asymmetric motions. *Phys. Fluids A* 1 (1989) 61–76.
7. C. Maul and S. Kim, Image systems for a stokeslet inside a rigid spherical container. *Phys. Fluids A* 6 (1994) 2221–2223.
8. S.F.J. Butler, A note on Stokes's stream function for motion with a spherical boundary. *Proc. Camb. Phil. Soc.* 49 (1953) 169–174.
9. W.D. Collins, Note on a sphere theorem for the axisymmetric Stokes flow of a viscous fluid. *Mathematika* 5 (1958) 118–121.
10. D. Palaniappan, S.D. Nigam, T. Amaranath and R. Usha, Lamb's solution of Stokes's equations: a sphere theorem. *Q. J. Mech. Appl. Math.* 45 (1992) 47–56.
11. R. Shail and S.H. Onslow, Some Stokes flows exterior to a spherical boundary. *Mathematika* 35 (1988) 233–246.
12. S. Kim and S.J. Karrila, *Microhydrodynamics: Principles and Selected Applications*. Boston: Butterworth–Heinemann, (1991) 507 pp.
13. J. Happel and H. Brenner, *Low Reynolds Number Hydrodynamics*. The Hague: Martinus Nijhoff (1983) 553 pp.
14. Y.O. Fuentes and S. Kim, Parallel computational microhydrodynamics: communication scheduling strategies. *A.I.Ch.E. Journal* 38 (1992) 1059–1078.
15. F. Traenkle, M.D. Hill and S. Kim, Solving microstructure electrostatics on a proposed parallel computer. *Computers and Chemical Engineering* 19 (1995) 743–757.